High-Precision Tracking Differentiator via Generalized Discrete-Time Optimal Control

Hehong Zhang[a], Yunde Xie[b], Chao Zhai[c], Gaoxi Xiao[c,*],

[a] *Interdisciplinary Graduate School, Nanyang Technological University, Singapore*
[b] *Beijng Enterprises Holding Maglev Technology Development Company Limited, Beijing 10024, China*
[c] *School of Electrical and Electronic Engineering, Nanyang Technological University, Singapore*

Abstract

An enhanced discrete-time tracking differentiator (TD) with high precision based on discrete-time optimal control (DTOC) law is proposed. This law takes the form of state feedback for a double-integral system that adopts the Isochronic Region approach. There, the control signal sequence is determined by a linearized criterion based on the position of the initial state point on the phase plane. The proposed control law can be easily extended to the TD design problem by combining the first-state variable of the double-integral system with the desired trajectory. To improve the precision of the discretization model, we introduced a zero-order hold on the control signal. We also discuss the general form of DTOC law by analysing the relationship between boundary transformations and boundary characteristic points. After comparing the simulation results from three different TDs, we determined that this new TD achieves better performance and higher precision in signal-tracking filtering and differentiation acquisition than do existing TDs. For confirmation of its utility, we processed raw phasor measurement units data via the proposed TD. In the absence of complex power system modelling and historical data, it was verified that the proposed TD is suitable for applications of real-time synchrophasor estimations, especially when the states are corrupted by noise.

Keywords: tracking differentiator (TD), discrete-time optimal control (DTOC), tracking, filtering, differentiation acquisition, estimation.

1. Introduction

Differentiation of signals is commonly applied in control algorithms [1] [2]. For example, one can use the derivative control within a PID controller to overcome the overshoot of an under-damped second- or higher-order plant [3].

*Corresponding author

However, differential signals are prone to noise corruption and usually are not measurable. Thereofore, they must instead be evaluated by taking an approximate differentiation of a measurable signal instead [4]. This makes the controller vulnerable to high-frequency noises. To deal with this, great efforts have been devoted to designing new differentiators, such as the high-gain observer-based differentiator [5], linear time-derivative trackers [6], the finite-time-convergent differentiator [7] and the robust exact differentiator [8] [9] and so forth [10]-[12].

A noise-tolerant time optimal control (TOC)-based tracking differentiator (TD) was firstly proposed by Han [13] [14]. Here, we provide a brief outline for constructing that TD. The double-integral system is defined as $\dot{x}_1 = x_2$, $\dot{x}_2 = u$, where $|u| \leq r$, r is a constant constraint of the control input. The resulting feedback control law that drives the state from any initial point to the origin in the shortest time is $u = -r\text{sign}(x_1 - v + \frac{x_2|x_2|}{2r})$, where v is the desired value for x_1. Using this principle, one can obtain the desired trajectory and its derivative by solving the following differential equations:

$$\begin{cases} \dot{v}_1 = v_2, \\ \dot{v}_2 = -r\text{sign}(v_1 - v + \frac{v_2|v_2|}{2r}) \end{cases}$$

where v_1 is the desired trajectory and v_2 is its derivative.

The advantage of this TOC-based TD is that it sets a weak condition on the stability of the systems to be constructed for TD and requires a weak condition on the input [15]-[17]. Because most control algorithms are now implemented in discrete time domain, a closed-form discrete-time optimal control (DTOC) law is needed for constructing TD with such favourable characteristics. Direct digitization of a continuous TOC solution proves to be problematic in practice because of the high-frequency chattering of the control signals. The work of Han provides an alternative mathematical solution to the DTOC problem, known as *Fhan* [18]. It was constructed based on an idea that goes back to 1950s: the concept of isochronous region, for a discrete-time, double-integral plant [19]. Because it introduces a boundary layer around the switching curve of bang-bang control, *Fhan* resolves the long-standing issue of chattering in the control signal of a continuous TOC solution. This characteristic confers an advantage of smoothness to the DTOC-based TD when compared with a sliding-mode-based differentiator.

However, the boundary curves of that IR where the control signal takes on non-extreme values are determined by a nonlinear boundary transformation. This means taking on a non-extreme value of control signal needs carrying out a nonlinear boundary transformation operation inside that IR. This gives *Fhan* a complex structure with non-linear calculations, including square-root calculations. Consequently, the precision of a *Fhan*-based TD in signal-tracking and differentiation acquisition is affected when using the Euler fold line approach, where differentiation of a state variable is approximately determined by a rectangular formula. In addition, the differential signals "jump" when a simulation is performed.

To tackle the challenges faced by *Fhan*-based TD, a new TD based on a closed-form DTOC law is presented. The main contributions by this work are

two-fold. First, inside the IR where the control signals take on non-extreme values, we have introduced a linear criterion to determine the control signals according to the relative position between the initial state and the boundary characteristic points instead of using a non-linear boundary transformation. Further, we obtain a general form of DTOC law with which one can flexibly design a new algorithm by modifying the boundary characteristic points. By doing so, one can avoid complex calculations resulting from a non-linear boundary transformation. Second, to improve the precision of a TD in signal-tracking and differentiation acquisition, we have introduced a zero-order hold on the control signal to enhance the precision of the discretization model.

The rest of paper is organized as follows: the background of TOC for a continuous-time double-integral system and its problem on direction digitization are introduced in Section 2. The construction and discussion on the general form of DTOC law ~~is~~ presented in Section 3. In Section 4, comparison simulation results among three different TDs are presented to demonstrate the better performance of the proposed Fhh-based TD in signal-tracking filtering and differentiation acquisition, followed by experiment results on processing PMU raw data from real power systems. Finally, Section 5 concludes the paper.

2. Background

A good review of TOC has been presented by Berkovitz (2013) [20]. In particular, the TOC of a continuous-time double-integral system is defined as follows [21]:

$$\begin{cases} \dot{x}_1 = x_2, \\ \dot{x}_2 = u, |u| \leq r \end{cases} \tag{1}$$

where $x(t) = [x_1(t), x_2(t)]^T \in R^2$. The resulting control law that drives any initial state point to the origin in the minimum time is

$$u(x_1, x_2, r) = -r\text{sign}(\Gamma(x_1, x_2)) \tag{2}$$

where $\Gamma(x_1, x_2) = x_1 + \frac{x_2|x_2|}{2r}$ is the switching curve. ~~If we denote~~ $T(x_1, x_2)$ as the time that any state point $M(x_1, x_2)$ reaches the origin, then

$$T(x_1, x_2) = \frac{x_2}{r}s + \frac{2}{\sqrt{r}}\sqrt{\frac{x_2^2}{2r} + sx_1} \tag{3}$$

where $s = \text{sign}(\text{x}_1 + \frac{\text{x}_2|\text{x}_2|}{2\text{r}})$. For a continuous-time plant (1), we choose $T(x_1, x_2)$ as the Lyapunov function, such that

$$\begin{cases} \frac{\partial T}{\partial x_1} = \frac{s}{\sqrt{r}\sqrt{(x_2^2/2r)+sx_1}} \\ \frac{\partial T}{\partial x_2} = \frac{s}{r} + \frac{x_2/r}{\sqrt{r}\sqrt{(x_2^2/2r)+sx_1}} \\ \frac{dT}{dt} = \frac{\partial T}{\partial x_1}\dot{x_1} + \frac{\partial T}{\partial x_2}\dot{x_2} = -1 \end{cases}$$

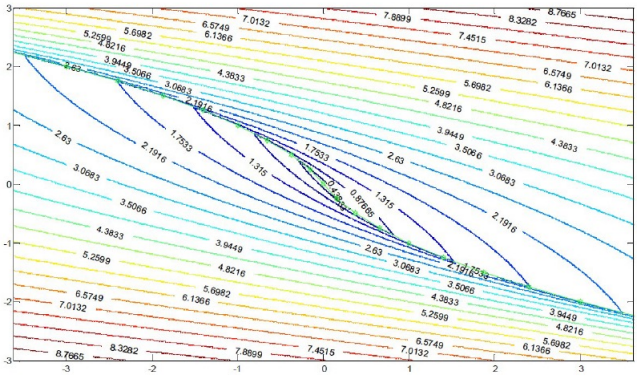

Figure 1: Time contour for reaching the origin

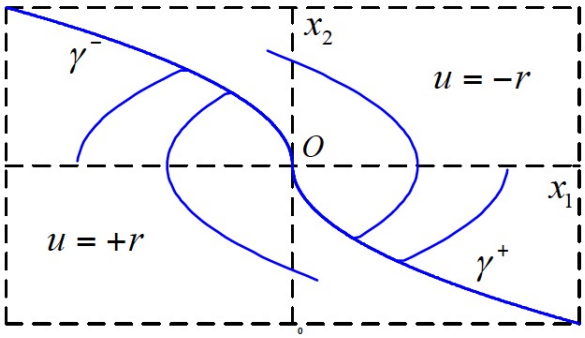

Figure 2: Switching curve and the optimal trajectories

Here, $T(x_1(t), x_2(t)) = -t + T(x_1(0), x_2(0))$, which indicates that any state can reach the origin along the optimal trajectory in finite time. The time contour of reaching the origin from any initial state is illustrated in Fig. 1. The switching curve $\Gamma = \gamma^+ \cup \gamma^-$ and the optimal trajectories are shown in Fig. 2.

In theory, this TOC takes on the switching curve as its sliding surface when the initial state is driven to that curve with an extreme value of the control signal [12] [23]. Therefore, this TOC method has the following advantages over a linear controller: 1) the state arrives at the steady state in minimal and finite time; and 2) superior disturbance rejection robustness against dynamic uncertainties [24]. It can also be easily extended to the tracking problem by replacing x_1 and x_2 in (2) with $x_1 - v$ and $x_2 - \dot{v}$, respectively. Here, v and $\dot{v}$ are the desired state trajectories. However, with the rapid development of computer control technology, most control algorithms are currently implemented within a discrete-time domain. Direct digitization of the continuous TOC solution has proven to be problematic in practice because of high-frequency chattering of the control signals [25].

For driving the initial state back to the origin in the continuous system described in (1), the control signal switches between its two extreme values around the switching curve $\Gamma(x_1, x_2)$ in (2). That is, when the initial state is located over the switching curve, the control signal takes on extreme values, i.e., $u = -r$; otherwise, the control signal takes on $u = +r$. That signal switches the sign after reaching the switching curve. For a continuous-time system, the control signal can switch instantaneously. For a discrete-time system, however, the process of sign-switching of the control signal occurs within the sampling period h [18]. During that process, the corresponding state sequences are located in a certain region (denoted as Ω) near the switching curve. The control signals for the state sequences in the region Ω are determined by a linearized criterion. Each signal varies from a certain positive (negative) value to a negative (positive) value when the control signal u passes from one side of the region Ω to the other. All of the initial state sequences that are outside of the region Ω when the control signal takes on extreme values, i.e., $u = +r$ or $u = -r$, are located at certain curves, referred to as boundary curves Γ_A and Γ_B, and the region Ω is surrounded by those curves. All states that correspond to $u = 0$ then constitute another curve that is referred to as the control characteristic curve Γ_C. We will introduce the above regions and curves in the next section.

3. Discrete-Time Tracking Differentiator

In this section, a new and simple tracking differentiator (TD) with high precision based on DTOC law is proposed. Precision of the discretization model is improved by introducing a zero-order hold on the control signal.

3.1. Problem Formulation

Given the double-integral state-space model in (1), we have

$$X(t) = e^{A(t-t_0)}X(t_0) + \int_{t_0}^{t} e^{A(t-\tau)}Bu(\tau)d\tau \tag{4}$$

where $A = \begin{pmatrix} 0 & 1 \\ 0 & 0 \end{pmatrix}$, $B = \begin{pmatrix} 0 \\ 1 \end{pmatrix}$ and $X(t) = [x_1(t), x_2(t)]^T \in R^2$. For discretization of (4), we take $t = (k+1)h$, $t_0 = kh$ and obtain

$$X[(k+1)h] = e^{Ah}X(kh) + \int_{kh}^{(k+1)h} e^{A[(k+1)h-\tau]}Bu(\tau)d\tau \tag{5}$$

If we let $\tau = kh + \sigma$ and substitute it into (5), then

$$X[(k+1)h] = e^{Ah}X(kh) + \int_{kh}^{(k+1)h} e^{A(h-\tau)}Bu(kh+\sigma)d\sigma \tag{6}$$

Furthermore,

$$X[(k+1)h] = \begin{bmatrix} 1 & h \\ 0 & 1 \end{bmatrix} X(kh) + \int_{0}^{h} \begin{bmatrix} h-\sigma \\ 1 \end{bmatrix} u(kh+\sigma)d\sigma \tag{7}$$

Using the Taylor expansion method, we ~~expanded~~ the item $u(kh+\sigma)$ at $t=kh$ to obtain

$$u(kh+\sigma)=\sum_{i=1}^{n}\frac{u^{(i)}(kh)}{i!}+O(\sigma^{n+1}) \tag{8}$$

If we let $n=0$ and ignore the higher-order terms, then

$$u(kh+\sigma)\approx u(kh) \tag{9}$$

Considering the zero-order hold on the control signal, by substituting (9) into (7), we have

$$x(k+1)=Ax(k)+Bu(k), |u(k)|\leq r \tag{10}$$

where $A=\begin{bmatrix}1 & h\\ 0 & 1\end{bmatrix}$, $B=\begin{bmatrix}h^2/2\\ h\end{bmatrix}$ and $x(k)=[x_1(k),x_2(k)]^T$. The objective here is to derive a TOC law directly within a discrete-time domain. ~~That~~ problem is defined as follows:

DTOC Law: Given the system (10) and its initial state $x(0)$, we can determine the control signal sequence, $u(0)$, $u(1)$, ..., $u(k)$, such that the state $x(k)$ is driven back to the origin in a minimum and finite number of steps, subject to the constraint of $|u(k)|\leq r$. That is, finding $u(k^*)$, $|u(k)|\leq r$, such that $k^*=\min\{k|x(k+1)=0\}$.

For a discrete-time system, the state is measured only at the sampling instant, $t=kh$, where h is the sampling period. If we treat the measurement, $x(kh)$, as though it were an initial condition, $x(0)$, then all we need to find is $u(0)$, as defined by **DTOC Law** at each sampling instant. This is repeated until the state reaches the origin.

~~For a discrete-time system, the state is measured only at the instants when $t=kh$, where h is the sampling period. If we treat the measurement $x(kh)$ as though it were an initial condition $x(0)$, then all we must determine is $u(0)$, as defined by **DTOC Law** at each sampling instant. This is repeated until the state reaches the origin.~~

The proposed DTOC law is based on IR, which is referred to as the $G(k)$ approach. ~~There~~, $G(k)$ denotes the set of states that, for any initial state inside a specific IR, at least one admissible control sequence exists, i.e., $u(0)$, $u(1)$,...,$u(k)$, that makes the solution of (10) satisfy $x(k+1)=0$. Note that the IR grows in volume as k increases, i.e., $G(k-1)\in G(k)$. The basic idea in deriving the DTOC law is to identify a control signal sequence for any $x(0)\in G(k)$ and $x(0)\notin G(k-1)$, such that the next state $x(1)$, calculated from the discrete-time double-integral system, satisfies $x(1)\in G(k-1)$. This process is divided into two tasks:

1. Determine the boundary curves (Γ_A and Γ_B) of IR by connecting the points of $G(k)$ to form the Region Ω, as well as the control characteristic curve (Γ_C), from which the state can be driven back to the origin in finite steps;

2. For any given initial condition $x(0)\in\Omega$ or $x(0)\notin\Omega$, find the corresponding control signal sequence as a function of $x(0)$.

3.2. Determination of Boundary Curves and Control Characteristic Curve

As mentioned above, all initial state sequences outside the region Ω when the control signal takes on extreme values, i.e., $u = +r$ or $u = -r$, are located at certain boundary curves Γ_A and Γ_B that surround the Region Ω. All states corresponding to $u = 0$ constitute the control characteristic curve Γ_C.

Boundary curves (Γ_A and Γ_B) for the IR are then determined by connecting the points of $G(k)$ to form the Region Ω as well as Γ_C.

For any initial state sequence, at least one admissible control sequence, $u(0)$, $u(1)$, ..., $u(k)$ can make the solution of (10) satisfy $x(k+1) = 0$. Under initial condition $x(0)$, that solution is

$$x(k+1) = A^{k+1}x(0) + \sum_{i=0}^{k} A^{k-i}Bu(i) \tag{11}$$

where $x(0) = [x_1(0), x_2(0)]^T$ and $i = 0, 1, 2, ..., k$. Therefore, $x(k+1) = 0$ and the initial condition satisfies

$$x(0) = -\sum_{i=0}^{k} A^{-i-1}Bu(i) \tag{12}$$

Based on ~~this~~ state back-stepping approach above, we can ~~then~~ determine Γ_A, Γ_B, and Γ_C as follows.

For any initial state located above the switching curve and entered into the region Ω, we ~~might~~ suppose that the control signal sequence in the first step takes on $u(0) = -\alpha_1 r$, where α_1 is a variable~~, and~~ from the second step on, the control sequence takes on $u(i) = +r$ $i = 1, 2, ..., k$. According to (12), we obtain:

$$\begin{bmatrix} x_1(0) \\ x_2(0) \end{bmatrix} = \begin{bmatrix} h^2 r(-\frac{\alpha_1}{2} + \frac{k}{2} + \frac{k}{2}(k+1)) \\ hr(\alpha_1 - k) \end{bmatrix} \tag{13}$$

Simplifying $x(0)$ into x and eliminating the variable k, we get

$$x_1 - \frac{x_2^2}{2r} + hx_2(\alpha_1 + 1) - \frac{\alpha_1(\alpha_1+1)}{2}rh^2 = 0 \tag{14}$$

Similarly, for any initial state located above the switching curve and entered into the region Ω, we ~~can~~ suppose that the control signal sequence in the first step takes on $u(0) = +\alpha_1 r$, where α_1 is a variable, and from the second step on, the control sequence takes on $u(i) = -r$ $i = 1, 2, ..., k$. Therefore,

$$\begin{bmatrix} x_1(0) \\ x_2(0) \end{bmatrix} = \begin{bmatrix} h^2 r(\frac{\alpha_1}{2} - \frac{k}{2} - \frac{k}{2}(k+1)) \\ hr(-\alpha_1 + k) \end{bmatrix} \tag{15}$$

Simplifying $x(0)$ into x and eliminating the variable k, we have

$$x_1 + \frac{x_2^2}{2r} + hx_2(\alpha_1 + 1) + \frac{\alpha_1(\alpha_1+1)}{2}rh^2 = 0 \tag{16}$$

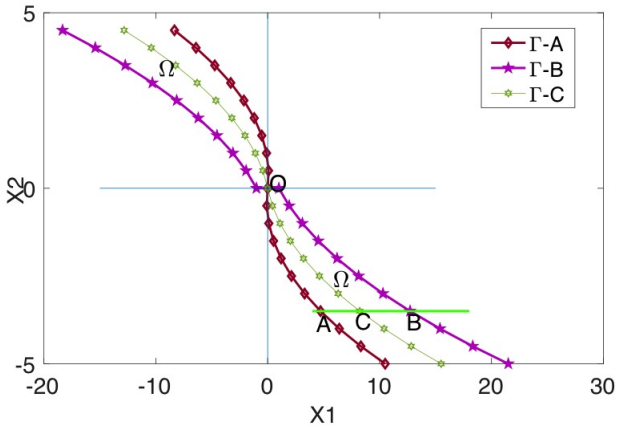

Figure 3: Illustrations of Γ_A, Γ_B, Γ_C and the region Ω.

Furthermore, according to (8) and (10), we have

$$x_1 + \frac{x_2|x_2|}{2r} + hx_2(\alpha_1 + 1) + \frac{\alpha_1(\alpha_1 + 1)}{2} rh^2 \text{sign}(x_2) = 0 \tag{17}$$

The boundary curves and the control characteristic curve depend upon the value of the control signal sequence in the first step, that is, the value of α_1. When $\alpha_1 = -1$, ~~then~~ boundary curve Γ_A is $x_1 + \frac{x_2|x_2|}{2r} = 0$. When $\alpha_1 = 0$, we obtain the control characteristic curve $\Gamma_C : x_1 + \frac{x_2|x_2|}{2r} + hx_2 = 0$. When $\alpha_1 = 1$, the boundary curve Γ_B is $x_1 + \frac{x_2|x_2|}{2r} + 2hx_2 + rh^2\text{sign}(x_2) = 0$.

Those two boundary curves in the region Ω, as well as the control characteristic curve, are determined by the state back-stepping method. They are shown on the phase plane in Fig. 3.

3.3. Construction of the DTOC Law

~~Using~~ the boundary curves, the control characteristic curve, and the regions described above, we can then construct the DTOC law. As shown in Fig. 3, we assume that, for any initial state $M(x_1, x_2)$ in the fourth quadrant $(x_1 > 0, x_2 < 0)$, there is an auxiliary line $x_2 = x_2(M)$ that intersects with the boundary curves and the control characteristic curve at points A, C, and B (in the direction of x_1). Their x-axis values x_A, x_B, and x_C are

$$\begin{cases} x_A = \frac{x_2^2}{2r} \\ x_B = \frac{x_2^2}{2r} + 2h|x_2| + h^2 r \\ x_C = \frac{x_2^2}{2r} + h|x_2| \end{cases} \tag{18}$$

For any initial state $M(x_1, x_2)$ satisfying $x_1 < x_A$ or $x_1 > x_B$, the control signal is taken as $u = +r$ or $u = -r$. For any initial state $M(x_1, x_2)$ that

satisfies $x_1 \in [x_A, x_C]$, the control signal can be determined as follows:

$$u = -r\alpha \text{sign}(x_2) \tag{19}$$

where $\alpha = \frac{x_C - x_1}{x_C - x_A}$. For any initial state $M(x_1, x_2)$ satisfying $x_1 \in [x_C, x_B]$, the control signal is calculated as:

$$u = r\beta \text{sign}(x_2) \tag{20}$$

where $\beta = \frac{x_1 - x_C}{x_B - x_C}$. When the initial state $M(x_1, x_2)$ is in the second quadrant, the control signal sequence can be constructed similarly.

However, when the initial state $M(x_1, x_2)$ (located outside the region Ω) is in the first or third quadrant, ~~are~~ two different cases exist for choosing the control signal: (i) when $M(x_1, x_2)$ cannot be driven back to the origin within two steps, that is, the initial state does not satisfy the condition $x_1^2 + x_2^2 = 0$, let $u = -r\text{sign}(x_1 + hx_2)$; or (ii) when $M(x_1, x_2)$ can be driven back to the origin within two steps, the initial state $x(0)$ and the corresponding control signal sequence satisfy (12), i.e.,

$$\begin{cases} x_1(1) = x_1(0) + hx_2(0) + \frac{1}{2}h^2u(0) \\ x_2(1) = x_2(0) + hu(0) \\ x_1(2) = x_1(1) + hx_2(1) + \frac{1}{2}h^2u(1) \\ x_2(2) = x_2(1) + hu(1). \end{cases}$$

The corresponding control signals ~~are~~ derived as follows:

$$\begin{cases} u(0) = -\frac{2x_1(0) + 3hx_2(0)}{2h^2} \\ \\ u(1) = -\frac{2x_1(1) + 3hx_2(1)}{2h^2}. \end{cases} \tag{21}$$

The region in which any $x(0)$ can be driven back to the origin within two steps, denoted as Ω_2 (see Fig. 4), is surrounded by two pairs of parallel lines $2x_1 + hx_2 = \pm 2h^2 r$ and $2x_1 + 3hx_2 = \pm h^2 r$.

Thus, any initial state $M(x_1, x_2)$ on the $x_1 - x_2$ plane can be driven back to the origin in a minimum and finite number of steps ~~according to~~ the control signal sequence above. The complete DTOC law is ~~then~~ presented as follows:

Step 1: Setting $y_1 = 2x_1 + 3hx_2, y_2 = 2x_1 + hx_2$, if $|y_1| > 2h^2 r$ or $|y_2| > 2h^2 r$, then $M(x_1, x_2)$ cannot be driven back to the origin within two steps, i.e., $M(x_1, x_2) \notin \Omega_2$, go to next step; otherwise, go to Step 5;

Step 2: If the initial state $M(x_1, x_2)$ satisfies $x_1 x_2 \geq 0$ and $M(x_1, x_2) \notin \Omega_2 \cup \Omega$, then the control signal takes on $u = -r\text{sign}(x_1 + x_2)$;

Step 3: Determine the boundary of the region Ω, i.e., $x_A = \frac{x_2^2}{2r}$, $x_B = \frac{x_2^2}{2r} + 2h|x_2| + h^2 r$ and $x_C = \frac{x_2^2}{2r} + h|x_2|$;

Step 4: If $|x_1| > x_B$, then the control signal takes on $u = -r\text{sign}(x_1)$; if $|x_1| < x_A$, then the control signal takes on $u = r\text{sign}(x_1)$; if $x_1 \in [x_A, x_C]$, the control signal takes on $u = -r\alpha\text{sign}(x_2)$; if $x_1 \in [x_C, x_B]$, we have $u = +r\beta\text{sign}(x_2)$, where $\alpha = \frac{x_C - x_1}{x_C - x_A}$ and $\beta = \frac{x_1 - x_C}{x_B - x_C}$;

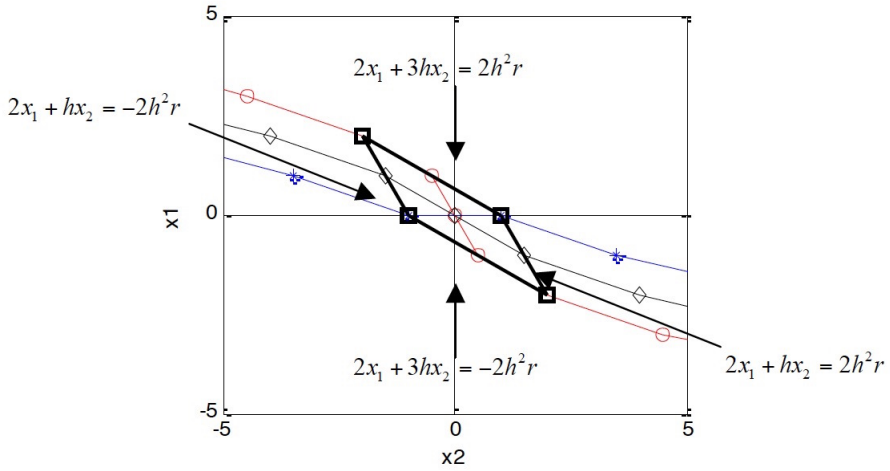

Figure 4: Illustration of Ω_2.

Step 5: If the initial state $M(x_1, x_2) \in \Omega_2$, then the control signal takes on $u(i) = \frac{2x_1(i)+3hx_2(i)}{2h^2}$, where $i = 0, 1$;

Step 6: The algorithm ends.

~~From~~ the deduction above, we ~~then~~ obtain the mathematical derivation of a closed-form DTOC law (**DTOC Law**) as a function of x_1, x_2, r, and h, denoted as $u(k) = Fhh(x_1(k), x_2(k), r, h)$.

Remark 1: Unlike the well-known bang-bang control for continuous-time plants, this closed-form time optimal control applies to discrete-time plants. The closed-form non-linear state feedback clearly demonstrates that TOC in discrete time is not necessarily bang-bang control, i.e., the control signal does not always take on extreme values. In fact, this characteristic makes our new control law advantageous ~~in fields of engineering~~ because it resolves the long-standing issue of chattering in the control signal. Therefore, our new approach can be used to design controllers, observers, and exact differentiators.

3.4. Discussion on General Form of DTOC Law

The traditional DTOC law ($Fhan$) of the TD is determined by comparing the position of the initial state with the IR through non-linear boundary transformation functions. In contrast, our proposed DTOC law (Fhh) is created by the boundary curves, a control characteristic curve, and three corresponding boundary characteristic points (x_A, x_B, and x_C). This produces a one-to-one correspondence between boundary transformation functions and boundary characteristic points. Therefore, obtaining the general form of DTOC laws can be accomplished flexibly by ~~using modified~~ points.

According to [11], the boundary functions of $Fhan$ are

$$\begin{cases} x_2 + \frac{1}{2}(\sqrt{\phi^2 h^2 r^2 + 8r|y|} - \phi hr)\text{sign}(y) = \phi hr \\ x_2 + \frac{1}{2}(\sqrt{\phi^2 h^2 r^2 + 8r|y|} - \phi hr)\text{sign}(y) = -\phi hr \\ y = x_1 + \lambda h x_2, \phi = 1.0, \lambda = 1.0 \end{cases} \tag{22}$$

Using the boundary transformation method, we ~~achieve~~ the corresponding boundary characteristic points as follows:

$$\begin{cases} x_A = \frac{x_2^2}{2r} + \frac{1}{2}h|x_2| \\ x_B = \frac{x_2^2}{2r} + \frac{5}{2}h|x_2| + h^2 r \\ x_C = \frac{x_2^2}{2r} + \frac{3}{2}h|x_2|. \end{cases} \tag{23}$$

For the proposed Fhh law, the boundary characteristic points are

$$\begin{cases} x_A = \frac{x_2^2}{2r} \\ x_B = \frac{x_2^2}{2r} + 2h|x_2| + h^2 r \\ x_C = \frac{x_2^2}{2r} + h|x_2| \end{cases} \tag{24}$$

The boundary functions of that law are presented as follows:

$$\begin{cases} x_2 + \frac{1}{2}(\sqrt{\phi^2 h^2 r^2 + 8r|y|} - \phi hr)\text{sign}(y) = \phi hr \\ x_2 + \frac{1}{2}(\sqrt{\phi^2 h^2 r^2 + 8r|y|} - \phi hr)\text{sign}(y) = -\phi hr \\ y = x_1 + \lambda h x_2, \phi = 0.5, \lambda = 0.5 \end{cases} \tag{25}$$

From ~~this~~ analysis, we ~~can~~ conclude that the boundary transformation of DTOC law is not unique. The switching curve of the proposed DTOC law is the same as the switching curve identified in the continuous-time case, which implies that the $Fhan$ law is not an optimal algorithm as claimed. In fact, ~~many~~ different types of tracking differentiators are possible based on various boundary transformations. For example, one can easily obtain other DTOC laws by modifying the boundary characteristic points, which then result in different precision in signal tracking and differentiation acquisition. Because of this, the range of laws ~~might simply~~ be considered variants of each other.

4. Numerical Simulations and PMU data Processing

We ran numerical simulations to compare the performance of the proposed differentiator with that of the existing ones for signal-tracking filtering and differentiation acquisition. We also conducted experiments using this model-free TD to filter and estimate phasor measurement unit (PMU) data from the field.

Based on the control law Fhh, we constructed the following TD:

$$\begin{cases} u(k) = Fhh(x_1(k) - v(k), x_2(k), r, c_0 h) \\ x_1(k+1) = x_1(k) + hx_2(k) + \frac{1}{2}h^2 u(k) \\ x_2(k+1) = x_2(k) + hu(k) \end{cases} \tag{26}$$

where r is the quickness factor, c_0 is the filtering factor, h is the sampling period, and v is the given signal.

4.1. Comparison Simulations

DI. Tracking differentiator based on $Fhan$ [13].

$$\begin{cases} u(k) = Fhan(x_1(k) - v(k), x_2(k), r, c_0 h), \\ x_1(k+1) = x_1(k) + hx_2(k), \\ x_2(k+1) = x_2(k) + hu(k), |u(k)| \leq r \end{cases}$$

DII. Tracking differentiator based on Ftd [11].

$$\begin{cases} u(k) = Ftd(x_1(k) - v(k), x_2(k), r, c_0 h) \\ x_1(k+1) = x_1(k) + hx_2(k) \\ x_2(k+1) = x_2(k) + hu(k), |u(k)| \leq r \end{cases}$$

DIII. Tracking differentiator based on Fhh.

$$\begin{cases} u(k) = Fhh(x_1(k) - v(k), x_2(k), r, c_0 h) \\ x_1(k+1) = x_1(k) + hx_2(k) + \frac{1}{2}h^2 u(k) \\ x_2(k+1) = x_2(k) + hu(k), |u(k)| \leq r \end{cases}$$

For these simulations, we selected the step function and sinusoidal signal as our input signal sequences, setting the same initial value ($x_1(0) = 0$, $x_2(0) = 2$) for all of the simulations. For the three differentiators, we also set the same parameters: sampling period, $h = 0.005s$; quickness factor, $r_0 = 500$; and filtering factor, $c_0 = 5$. We ~~then~~ plotted the results ~~after comparing the~~ signal-tracking filtering and differentiation acquisition.

Figures 5 7 and 8 revealed that three different TDs could quickly track the input signals without overshooting and chattering. Our proposed Fhh-based TD proved to be the most rapid in signal-tracking. As shown in Figures ,6 9 and 10, although the $Fhan$-based TD was, to some extent, capable of producing good differential signals, some intermittent jumps occurred in differentiation acquisition. In contrast, the proposed Fhh-based TD avoided such jumps and obtained the highest precision of differential signals within the shortest time.

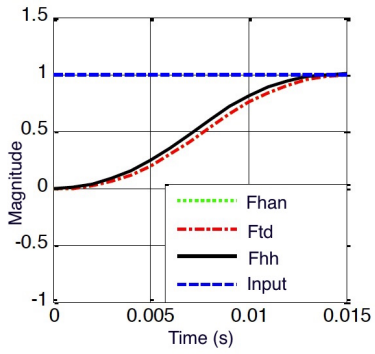

Figure 5: Outputs of signal-tracking filtering for step input

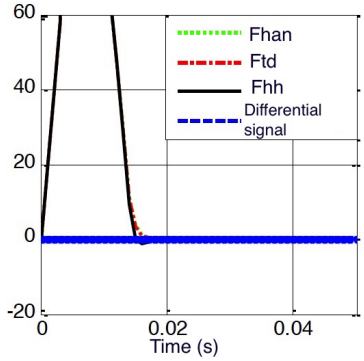

Figure 6: Outputs of differentiation acquisition for step input

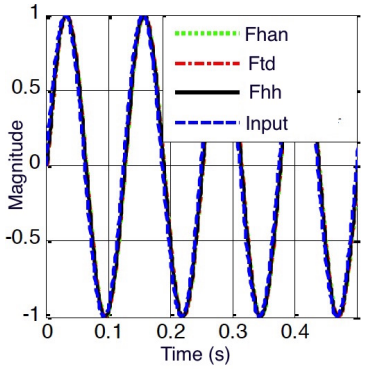

Figure 7: Outputs of signal-tracking filtering for sinusoidal signal input

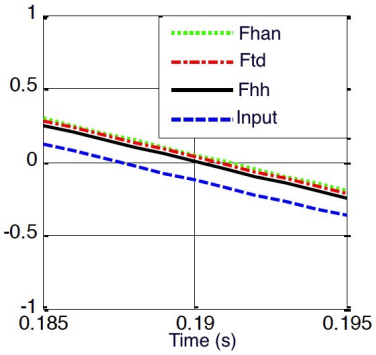

Figure 8: Partial enlargement of signal-tracking filtering for sinusoidal signal input

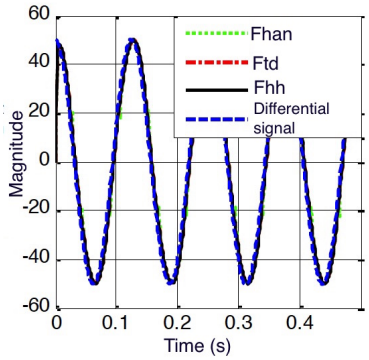

Figure 9: Outputs of differentiation acquisition for sinusoidal signal input

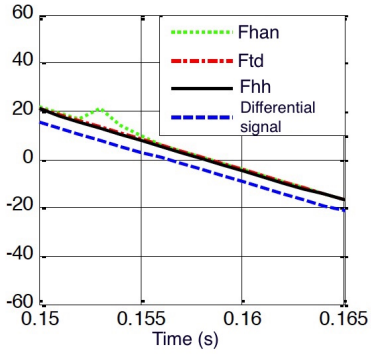

Figure 10: Partial enlargement of differentiation acquisition for sinusoidal signal input

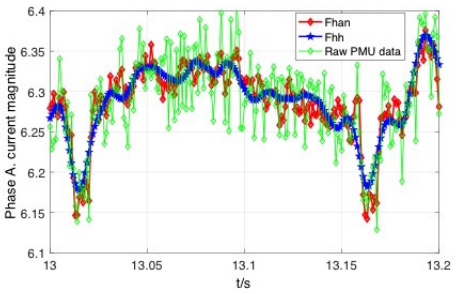

Figure 11: Output of current magnitude SE filtering using the real-time PMU data.

To quantify the differences among these differentiators, settling time (3%), steady-state error and the RMS error are used as criteria for comparison, as shown in Table 1. In the table, the letter "T" stands for signal tracking while the letter "D" represents differentiation acquisition.

Table 1: Comparison of results among $Fhan$, Ftd, and Fhh

Algorithm	Input	Settling Time (s)	Steady-state error (rev)	RMS error (rad)
$Fhan$	step function	0.015(T),0.018(D)	1.87×10^{-2}(T),2.45×10^{-2}(D)	0.236(T),0.265(D)
Ftd		0.015(T),0.018(D)	1.83×10^{-2}(T),2.41×10^{-2}(D)	0.233(T),0.261(D)
Fhh		0.012(T),0.016(D)	3.45×10^{-3}(T),3.67×10^{-3}(D)	0.114(T),0.118(D)
$Fhan$	sinusoidal signal	0.02(T),0.03(D)	0.025(T),0.088(D)	0.323(T),0.378(D)
Ftd		0.018(T),0.028(D)	0.023(T),0.086(D)	0.322(T),0.376(D)
Fhh		0.01(T),0.02(D)	0.018(T),0.065(D)	0.265(T),0.286(D)

The data displayed in Table 1 indicated that, based on discrete-time optimal control, the tracking differentiator **DIII** achieved better performance and higher precision in signal-tracking filtering and differentiation acquisition when compared with the other two differentiators.

4.2. PMU data Processing

A real-time, accurate state estimation (SE) is crucial if we are to enhance the effectiveness of system utilization, ensure the security of supply, and prevent blackouts [26]. Driven by these concerns, an increasing number of PMUs are being deployed in power systems. These devices collect accurate and synchronized voltage/current phasors, making them capable of directly measuring the power-system state [27]. Here, we used real-time PMU data to compare SE filtering between our proposed discrete TD and the $Fhan$-based TD.

The raw data, including current and voltage phasors, were recorded during normal operations at a 20-KV power plant in Jiangsu Province, China. The sampling frequency was 4960 Hz. For this processing, we set the same parameters for both TDs: sampling period, $h = 0.001s$; quickness factor, $r_0 = 800$; and filtering factor, $c_0 = 8$. The raw PMU data and corresponding processing results are plotted in Fig. 11. From Fig. 11, we can see that, by using the proposed TD, the SE filtering output was more effective and performance was better than the $Fhan$-based TD.

From Fig. 11, we can see that ~~using~~ the proposed TD can obtain effective state estimation filtering output and perform better than $Fhan$ based TD.

5. Conclusions

We proposed a generalized discrete-time optimal control law-based tracking differentiator that incorporates a zero-order hold on the control signal to improve the precision of the discretization model. This closed-form, nonlinear state feedback clearly demonstrates that time optimal control in discrete time is not necessarily bang-bang control. Therefore, that characteristic makes the new control law advantageous in engineering applications. Based on boundary transformation analysis, we determined that this proposed DTOC law is a general one, which suggests that one can easily construct other DTOC laws with different features ~~if~~ the boundary characteristic points ~~are modified~~. ~~Our numerical~~ simulation results indicated that, when compared with two existing differentiators, the proposed TD achieves better performance and higher precision in signal-tracking filtering and differentiation acquisition. ~~Using~~ the proposed TD to filter the PMU data, we showed that ~~this method~~ is promising for realizing real-time synchrophasor estimation applications. Future work will include precision analysis ~~among~~ various TDs, estimation of the convergence time of different DTOC laws, and assessing the robustness of finite-time or ultimate boundedness for a class of perturbations.

Acknowledgment

This study is an outcome of the Future Resilient System (FRS) project at the Singapore-ETH Centre (SEC), which is funded by the National Research Foundation of Singapore (NRF) under its Campus for Research Excellence and Technological Enterprise (CREATE) program. Part of this work is also supported by the Ministry of Education (MOE), Singapore (Contract No. MOE 2016-T2-1-119) and Interdisciplinary Graduate School, Nanyang Technological University, Singapore.

References

[1] Levant A, Livne M. Exact differentiation of signals with unbounded higher derivatives. IEEE Trans. Automat. Contr. 2012;57(4):1076-1080.

[2] Ang KH, Chong G, Li Y. PID control system analysis, design, and technology. IEEE Trans. Contr. Syst. Technol. 2005;13(4):559-576.

[3] Gao Z. From linear to nonlinear control means: A practical progression. ISA Trans. 2002;41(2):177-189.

[4] Wang Q, Lee T, Fung H, Bi Q, Zhang Y. PID tuning for improved performance. IEEE Trans. Contr. Syst. Technol. 1999;7(4):457-465.

[5] Ahrens JH, Khalil HK. High-gain observers in the presence of measurement noise: A switched-gain approach. Automatica 2009;45(4):936-943.

[6] Ibrir S. Linear time-derivative trackers. Automatica 2004; 40(3):397-405.

[7] Wang X, Chen Z, Yang G. Finite-time-convergent differentiator based on singular perturbation technique. IEEE Trans. Automat. Contr. 2007;52(9):1731-1737.

[8] Davila J, Fridman L, Levant A. Second-order sliding-mode observer for mechanical systems. IEEE Trans Automat Contr. 2005;50(11):1785-1789.

[9] Levant A. Robust exact differentiation via sliding mode technique. Automatica 1998;34(3):379-384.

[10] Ngo NQ. A new approach for the design of wideband digital integrator and differentiator. IEEE Trans. Circuits Syst. II, Exp. Briefs. 2006;53(9):936-940.

[11] Zhang H, Xie Y, Xiao G, Zhai C. Closed-form solution of discrete-time optimal control and its convergence. IET Contr. Theory A 2017;12(3):413-418.

[12] Liu D, Zheng G, Boutat D, Liu HR. Non-asymptotic fractional order differentiator for a class of fractional order linear systems. Automatica 2017;78:61-71.

[13] Han J. From PID to active disturbance rejection control. IEEE Trans. Ind. Electron. 2009;56(3):900-906.

[14] Han J. The discrete form of the tracking differentiator. Syst. Sci. Math. Sci. 1999;19:268-273.

[15] Guo B, Zhao Z. The Tracking Differentiator (TD). Active Disturbance Rejection Control for Nonlinear Systems: An Introduction 2016;53-91.

[16] Xue W, Huang Y, Yang, X. What kinds of system can be used as tracking-differentiator. In: Proc. of the 29th Chinese Control Conference, July; 2010. p. 6113-6120.

[17] Utkin V, Lee, H. Chattering problem in sliding mode control systems. In: Proc. of the International Workshop on Variable Structure Systems; 2006. p. 346-350.

[18] Han J, Yuan L. The discrete form of tracking-differentiator. J. Syst. Sci. Math. Sci. 1999.

[19] Gao Z. On discrete time optimal control: A closed-form solution. In: Proc. of the American Control Conference; 2004. p. 52-58.

[20] Berkovitz LD. Optimal control theory (Vol. 12). Springer Science and Business Media 2013.

[21] Kirk DE. Optimal control theory: an introduction. Courier Corporation 2012.

[22] Kalaykov I, Iliev B. Time-optimal sliding mode control of robot manipulator. In: Proc. of the 26th Annual Conference of the IEEE Industrial Electronics Society; 2000. p. 265-270.

[23] Iliev B, Kalaykov, I. Minimum-time sliding mode control for second-order systems. In: Proc. of the 2004 American Control Conference; 2004. p. 626-631.

[24] Chatchanayuenyong T, Parnichkun, M. Neural network based-time optimal sliding mode control for an autonomous underwater robot. Mechatronics 2006;16(8):471-478.

[25] Zhang H, Xie Y, Xiao G, Zhai C, Kang H, Tang J. Tracking Differentiator via Time Criterion. In: Proc. of the 2018 American Control Conference; 2018.

[26] Dasgupta S, Paramasivam M, Vaidya U, Ajjarapu V. Real-time monitoring of short-term voltage stability using PMU data. IEEE Trans. Power Syst. 2013;28(4):3702-3711.

[27] Zhou N, Meng D, Huang Z, Welch G. Dynamic state estimation of a synchronous machine using PMU data: A comparative study. IEEE Trans Smart Grid. 2015;6(1):450-460.